Oscillating flow of a compressible fluid through deformable pipes and pipe networks: wave propagation phenomena.

Yves Bernabé,

Earth, Atmospheric and Planetary Sciences Department, MIT

Acknowledgements: This work was partially funded by the US Department of Energy under grant DE-FG01-97ER14760.

Introduction

Time-dependent flow of interstitial fluid can potentially provide more information about the structure of porous media than steady-state flow. For example, transient and oscillating flow methods have been used in the laboratory to measure permeability and storativity of rock samples simultaneously [e.g., *Hsieh, et al.*, 1981; *Neuzil, et al.*, 1981; *Fischer*, 1992; *Fischer and Paterson*, 1992]. However, these methods rely on the assumption that the medium investigated is homogeneous. As a consequence, they fail to properly explain certain features observed in heterogeneous media. For instance, AC flow through a strongly heterogeneous medium depends on frequency [e.g., *Bernabé, et al.*, 2004; *Song and Renner*, 2006]. Even in homogeneous media, frequency-dependence arises from a transition from viscosity-controlled flow at low frequencies to inertia-controlled flow at high frequencies [e.g., *Johnson, et al.*, 1987]. In most work on frequency-dependent, AC permeability, the interstitial fluid is supposed to be incompressible and the pores rigid. One important consequence is that fluid flow waves cannot propagate in the porous medium under these conditions. To clarify this statement, let's consider a semi-infinite, rigid pipe saturated with an incompressible fluid. A fluid pressure oscillation at the pipe entrance produces an oscillating flow along the pipe, which, because of mass conservation and complete absence of storage, is independent on distance from the pipe entrance. In other words, a pressure disturbance and the associated flow are instantaneously transmitted from the pipe entrance to infinity. In contrast, studies of blood circulation through elastic arteries [e.g., *Zamir*, 2000] show that the entire body of fluid does not move in unison as in a rigid pipe. Fluid flow waves travel along the elastic arteries with a finite velocity. These waves are dispersive and attenuated. Their existence has far-reaching consequences since wave reflections and interferences greatly affect blood flow in the artery tree [e.g., *Duan and Zamir*, 1995; *Zamir*, 1998, 2000; *Wang and Parker*, 2004]. Logically, fluid flow waves must also occur in saturated pipe networks and, by extension, in porous media, provided the interstitial fluid is compressible and/or the porous medium is deformable. The purpose of this work is to derive a flow wave propagation model for a single pipe and use it to investigate flow waves through pipe networks.

AC flow of compressible fluid through a single infinitely long pipe

Notations: r, z, θ cylindrical coordinates

$u(r,z,t)$ axial $v(r,z,t)$ radial velocity in fluid

$p(r,z,t)$ pressure variation with respect to constant back pressure

$x(r,z,t)$ axial $y(r,z,t)$ radial displacement in solid

Main assumption: Long-wave approximation (wavelength λ >> pipe radius R, and/or, wave-speed c >> average flow velocity).

1. Rigid pipe

Continuity equation: $\beta \frac{\partial p}{\partial t} + \frac{\partial u}{\partial z} + \frac{\partial v}{\partial r} + \frac{v}{r} = 0$ (with $\beta = \frac{1}{\rho}\frac{\partial \rho}{\partial p}$)

Navier-Stokes equations: $\rho \frac{\partial u}{\partial t} = -\frac{\partial p}{\partial z} + \eta\left(\frac{\partial^2 u}{\partial r^2} + \frac{1}{r}\frac{\partial u}{\partial r}\right)$

$\rho \frac{\partial v}{\partial t} = -\frac{\partial p}{\partial r} + \eta\left(\frac{\partial^2 v}{\partial r^2} + \frac{1}{r}\frac{\partial v}{\partial r} - \frac{v}{r^2}\right)$ (with η viscosity).

Solutions are axially traveling fluid flow waves [e.g., *Zamir,* 2000]:

$u(r,z,t) = U(r)\, e^{-i\omega(t - z/c)}$

$v(r,z,t) = V(r)\, e^{-i\omega(t - z/c)}$

$p(r,z,t) = P(r)\, e^{-i\omega(t - z/c)}$ (with c complex wave-speed).

$$P(r) \approx B$$

$$U(r) = \frac{B}{\rho c}\left(1 - \frac{J_0(\kappa r)}{J_0(\kappa R)}\right)$$

$$V(r) = \frac{rB\kappa^2\eta}{\rho^2 c^2 J_0(\kappa R)}\left(\frac{J_1(\kappa r)}{\kappa r} - \frac{J_1(\kappa R)}{\kappa R}\right)$$

(with B an integration constant, $\kappa = \sqrt{\frac{i\omega\rho}{\eta}}$ and $c_0 = 1/\beta\rho$ the fluid sound velocity)

Dispersion equation: $$c^2 = c_0^2\left(1 - \frac{2\mathrm{J}_1(\kappa R)}{\kappa R \mathrm{J}_0(\kappa R)}\right)$$

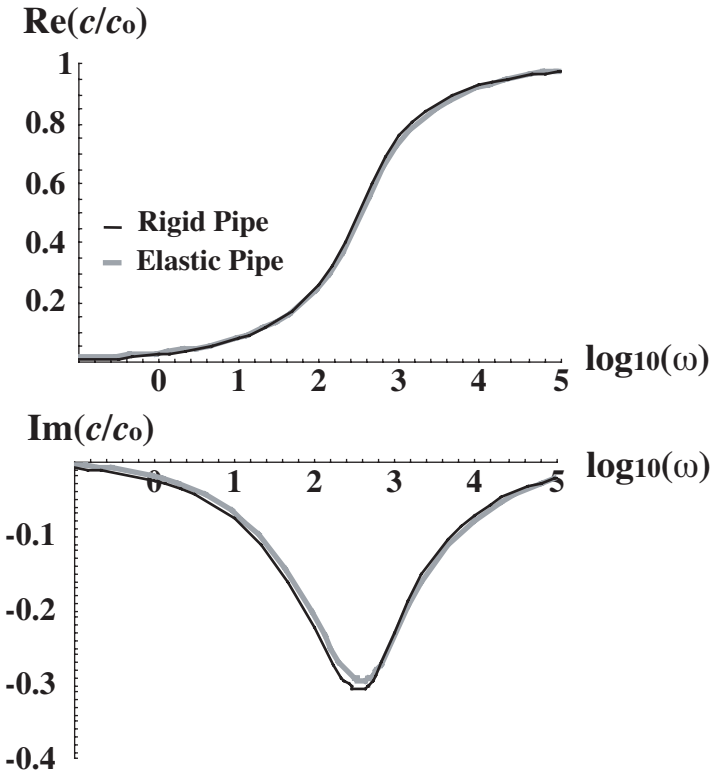

Axial volumetric flux $q(z,t) = Q\, e^{-i\omega(t - z/c)}$:

$$Q = \frac{-\pi R^2 B}{\rho c}\left(\frac{2\mathrm{J}_1(\kappa R)}{\kappa R \mathrm{J}_0(\kappa R)} - 1\right) = \frac{-\pi R^2 \nabla P}{\eta \kappa^2}\left(\frac{2\mathrm{J}_1(\kappa R)}{\kappa R \mathrm{J}_0(\kappa R)} - 1\right) \qquad \text{(with } \nabla P = i\omega B/c \text{)}$$

2. Elastic pipe

Elastic potentials in solid:

$$x(r,z,t) = \frac{\partial \Phi}{\partial z} + \frac{\partial \Psi}{\partial r} + \frac{\Psi}{r}, \text{ and, } y(r,z,t) = \frac{\partial \Phi}{\partial r} - \frac{\partial \Psi}{\partial z}$$

Force balance equations:

$$\frac{\partial^2 \Phi}{\partial r^2} + \frac{1}{r}\frac{\partial \Phi}{\partial r} + \frac{\partial^2 \Phi}{\partial z^2} = \frac{1}{V_P^2}\frac{\partial^2 \Phi}{\partial t^2}$$

$$\frac{\partial^2 \Psi}{\partial r^2} + \frac{1}{r}\frac{\partial \Psi}{\partial r} - \frac{\Psi}{r^2} + \frac{\partial^2 \Psi}{\partial z^2} = \frac{1}{V_S^2}\frac{\partial^2 \Psi}{\partial t^2}$$

Solutions:

$\Phi(r,z,t) = C\, K_0(lr)\, e^{-ik(ct-z)}$ (with $k = \omega/c$ and $l^2 = k^2\,(1-c^2/V_P^2)$)

$\Psi(r,z,t) = D\, K_1(mr)\, e^{-ik(ct-z)}$ (with $m^2 = k^2\,(1-c^2/V_S^2)$)

Dispersion equation:

$$c^4 - c^2\left(\frac{2J_1(\kappa R)}{\kappa R J_0(\kappa R)}\frac{\rho}{\rho_S}c_0^2 + c_0^2 + 2V_S^2\right) + 2V_S^2 c_0^2\left(1 - \frac{2J_1(\kappa R)}{\kappa R J_0(\kappa R)}\right) = 0$$

Fluid velocity:

$$U(r) = \frac{B}{\rho c}\left(1 - \frac{\kappa R J_0(\kappa r)}{2J_1(\kappa R)}\left[1 - \frac{c^2}{c_0^2} + \frac{c^2}{V_S^2}\frac{\rho}{\rho_S}\right]\right)$$

$$V(r) = \frac{i\omega B}{2\rho}R\left(\frac{J_1(\kappa r)}{J_1(\kappa R)}\left[\frac{1}{c^2} - \frac{1}{c_0^2} + \frac{1}{V_S^2}\frac{\rho}{\rho_S}\right] - \frac{r}{R}\left[\frac{1}{c^2} - \frac{1}{c_0^2}\right]\right)$$

Fluid volumetric flux:

$$Q = -\frac{\pi R^2 B}{\rho c}\left(\frac{\rho c_0^2}{\rho_S V_S^2} - 1\right)\frac{c^2}{c_0^2}$$

AC flow of compressible fluid through a single pipe of finite length *L*

Flow wave reflections and interferences

The pressure inside the pipe is sum of two waves traveling in opposite directions:

$$p(z,t) = B^{+}\mathrm{e}^{-\mathrm{i}\omega(t-z/c)} + B^{-}\mathrm{e}^{-\mathrm{i}\omega(t+z/c)}$$

$$B^{+} = \frac{P_D - P_U\mathrm{e}^{-\mathrm{i}\omega L/c}}{\mathrm{e}^{\mathrm{i}\omega L/c} - \mathrm{e}^{-\mathrm{i}\omega L/c}}$$

$$B^{-} = \frac{P_U\mathrm{e}^{\mathrm{i}\omega L/c} - P_D}{\mathrm{e}^{\mathrm{i}\omega L/c} - \mathrm{e}^{-\mathrm{i}\omega L/c}}$$ (with P_U and P_D upstream and downstream amplitudes)

Volumetric flux $q(z,t)$ also sum of two traveling waves:

$$q(z,t) = Q^{+}\mathrm{e}^{-\mathrm{i}\omega(t-z/c)} + Q^{-}\mathrm{e}^{-\mathrm{i}\omega(t+z/c)}$$

$$Q_U = Q^{+} + Q^{-}, \text{ and, } Q_D = Q^{+}\mathrm{e}^{\mathrm{i}\omega L/c} + Q^{-}\mathrm{e}^{-\mathrm{i}\omega L/c}$$

$$Q_U = \frac{-\mathrm{i}\pi R^2}{\rho c}\left(\frac{P_U\cos(\omega L/c) - P_D}{\sin(\omega L/c)}\right)\left(\frac{2\mathrm{J}_1(\kappa R)}{\kappa R\mathrm{J}_0(\kappa R)} - 1\right)$$

$$Q_D = \frac{-\mathrm{i}\pi R^2}{\rho c}\left(\frac{P_U - P_D\cos(\omega L/c)}{\sin(\omega L/c)}\right)\left(\frac{2\mathrm{J}_1(\kappa R)}{\kappa R\mathrm{J}_0(\kappa R)} - 1\right)$$

Q_U and Q_D generally different owing to storage inside the pipe.

Identical only in the limit of an infinitesimally small pipe length.

Apparent upstream and downstream hydraulic conductivities

Steady-state flow: $K_{SS} = -\eta Q/\nabla P = \pi R^4/8$,

Incompressible AC flow: $K_{AC} = \frac{\pi R^2}{\kappa^2}\left(\frac{2\mathrm{J}_1(\kappa R)}{\kappa R\mathrm{J}_0(\kappa R)} - 1\right)$ [*Johnson, et al.,* 1987]

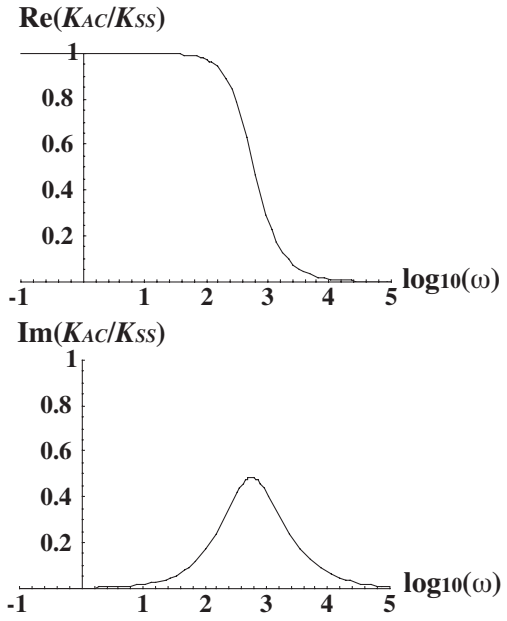

K_{AC}/K_{SS} for R = 100 μm.

Sharp transition between low- and high frequency regimes defines transition frequency $\omega_{V,I}$, which scales as $1/R^2$ [e.g., *Johnson, et al.*, 1987; *Charlaix, et al.*, 1988; *Bernabé*, 1997].

Compressible AC flow (flow wave propagation):

Different upstream and downstream hydraulic conductivities, K_U and K_D:

$$K_U = \frac{-\eta L Q_U}{P_D - P_U} \quad \text{and} \quad K_D = \frac{-\eta L Q_D}{P_D - P_U}$$

$$K_U = K_{AC}\frac{\omega L}{c}\frac{P_U \cos\left(\frac{\omega L}{c}\right) - P_D}{\sin\left(\frac{\omega L}{c}\right)\left(P_U - P_D\right)}$$

$$K_D = K_{AC}\frac{\omega L}{c}\frac{P_U - P_D \cos\left(\frac{\omega L}{c}\right)}{\sin\left(\frac{\omega L}{c}\right)\left(P_U - P_D\right)}$$

For an infinitesimally short pipe, $K_U \approx K_D \approx K_{AC}$ at all frequencies.

For finite pipe length, three regions:

(1) at low-frequencies, $K_U \approx K_D \approx K_{AC}$.

(2) at intermediate frequencies, wide irregular oscillations.

(3) at high-frequencies, $\mathrm{Re}(K_U/K_{AC}) \sim \omega^{1/2}$, $\mathrm{Im}(K_U/K_{AC}) \sim -\omega$ and $K_D/K_{AC} \sim 0$.

Transition frequency $\omega_{1,2}$ separating (1) and (2) scales roughly with $1/L$.

One important feature, $\mathrm{Re}(K_U/K_{SS})$ approaches a finite positive value K_∞/K_{SS} at high-frequencies (easily explained by remembering that $\mathrm{Re}(K_{AC}) \sim \omega^{-3/2}$ and $\mathrm{Im}(K_{AC}) \sim \omega^{-1}$).

Most striking, K_∞ tends to increase linearly with L and eventually becomes larger (possibly orders of magnitude larger) than the steady-state value K_{SS}.

To the contrary, K_D/K_{SS} vanishes in the high-frequency limit.

This very strong difference in high-frequency behavior between K_U and K_D is a consequence of fluid storage inside the pipe and obviously must increase linearly with the pipe length.

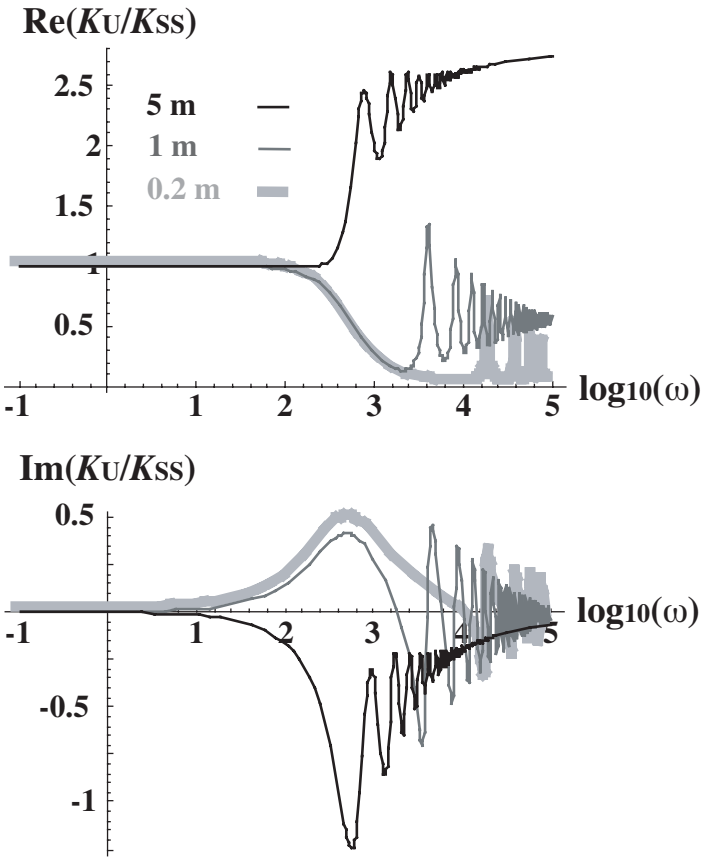

Real and imaginary parts of the normalized apparent conductivity K_U/K_{SS} for pipes with different lengths L (thick grey line, L = 0.2 m; thin grey line, L = 1 m; thin black line, L = 5 m; the pipe radius is equal to 100 μm). The frequencies are given in Hertz.

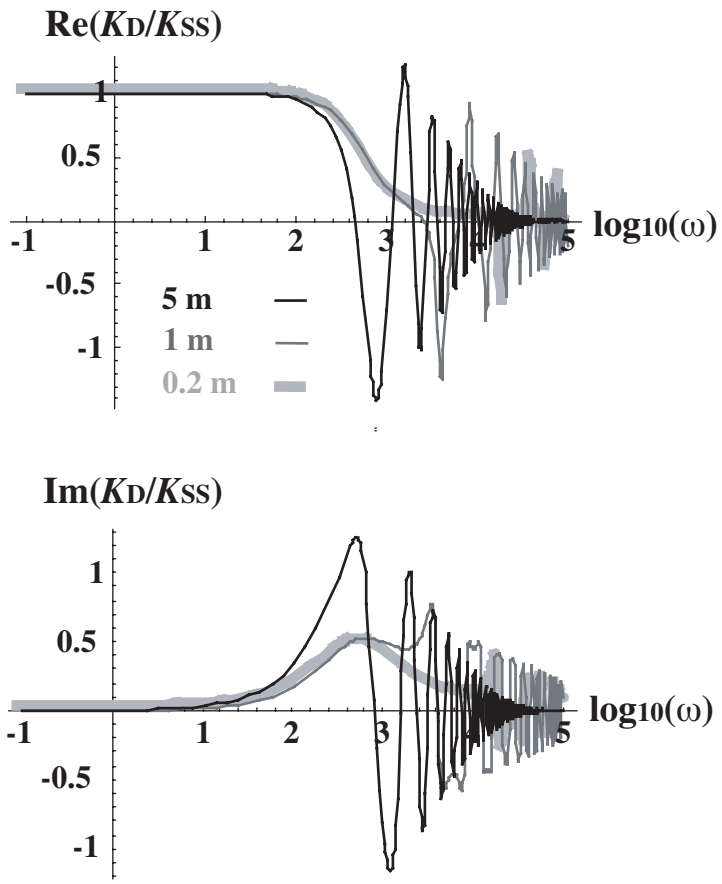

Real and imaginary parts of the normalized apparent conductivity K_D/K_{SS} for pipes with different lengths L (thin black line, L = 5 m; thin grey line, L = 1 m; thick grey line, L = 0.2 m; the pipe radius is equal to 100 μm).

AC flow through a two-dimensional network of pipes

Standard method for solving a stead-state flow problem on a pipe network can be used for an oscillating flow with a given frequency, except that a complex-valued matrix has to be inverted [*Bernabé*, 1997].

Goal was not to make realistic simulations of rocks but merely to illustrate the effect of wave reflections and interferences in relatively complex pipe systems. Hence, study is limited 10x10, 20x20 and 40x40 2D square networks, with semi-periodic boundary conditions and narrow pipe radius distribution (low level of heterogeneity).

Finally, global upstream and downstream conductivities (averaged over 10 realizations) calculated using previous definitions, in which Q_U and Q_D are the amplitudes of the total volumetric flux into/out of the upstream and downstream network sides, P_D–P_U = -1 is the global pressure amplitude difference, and, L refers to the total length of the network in the flow direction.

Next Figures show real and imaginary parts of K_U/K_{SS} as a function of frequency for 40x40 and 10x10 networks with different total length L.

Very similar to single pipe curves.

Transition frequency monotonically increasing function of the network length L and, therefore, likely related to wave reflection from the upstream and downstream ends of the network).

Internal reflections (i.e., from the ends of individual bonds) visible at high frequencies (but frequency resolution insufficient to accurately delineate the fluctuations of K_U/K_{SS}).

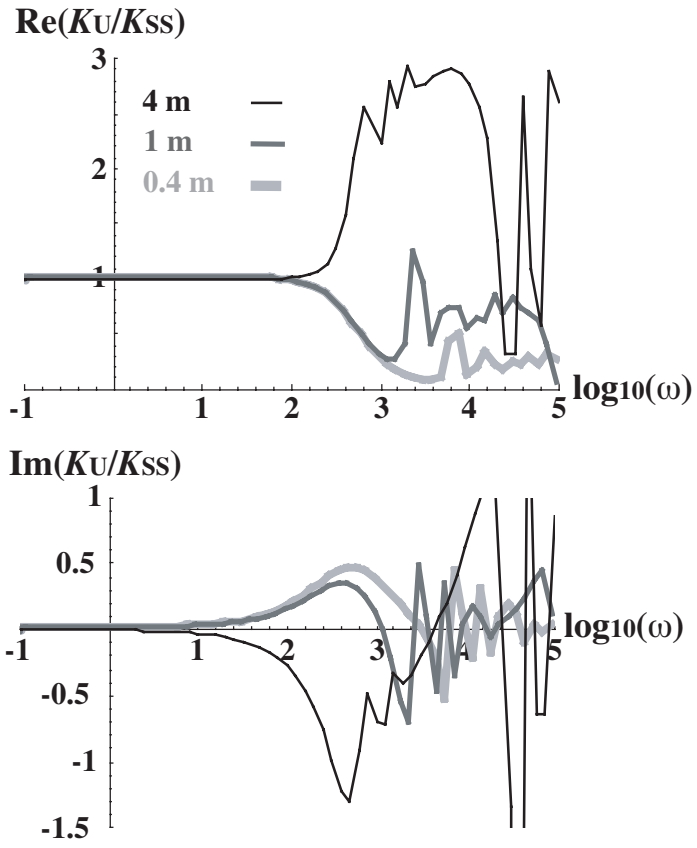

Real and imaginary parts of the normalized apparent permeability K_U/K_{SS} for 40x40 networks with different total lengths (thin, black line, L = 4 m; thicker, dark grey line, L = 1 m; thick, light grey line, L = 0.4 m; the mean radius of the pipes is 100 μm). Note that the diagrams show results of discrete calculations with an increment of 0.1 in $\log_{10}(\omega)$. The discrete data points are joined by straight lines for visibility.

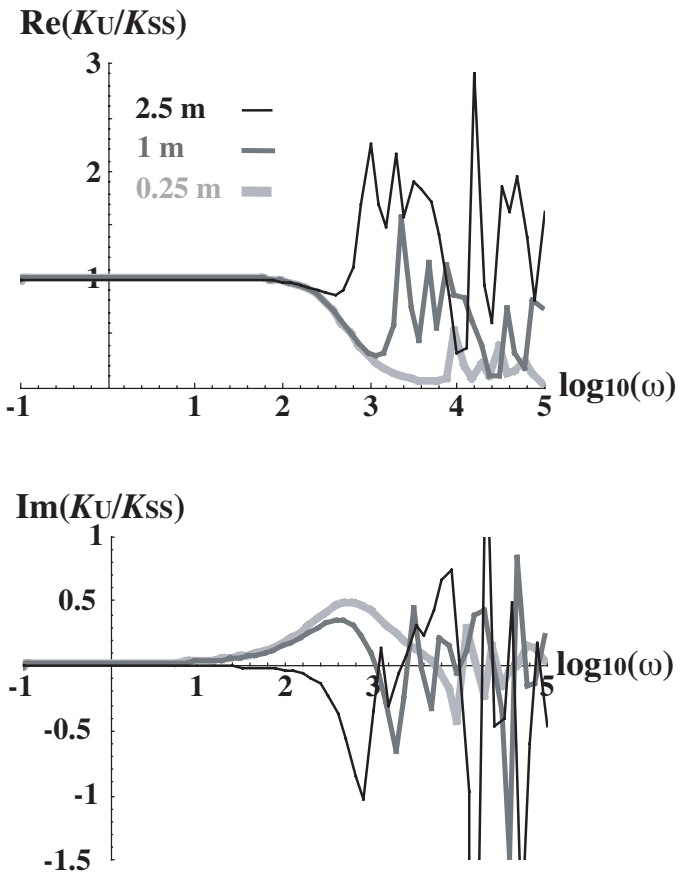

Real and imaginary parts of the normalized apparent permeability K_U/K_{SS} for 10x10 networks with different total lengths (thin, black line, L = 2.5 m; thicker, dark grey line, L = 1 m; thicker, light grey line, L = 0.25 m; the mean radius of the pipes is 100 μm).

Confirmation of role of wave reflections from the upstream and downstream ends:

40x40 and 10x10 networks with an identical total length.

20x20 networks containing a sharp discontinuity in the pipe radius distribution at mid-length in the flow direction.

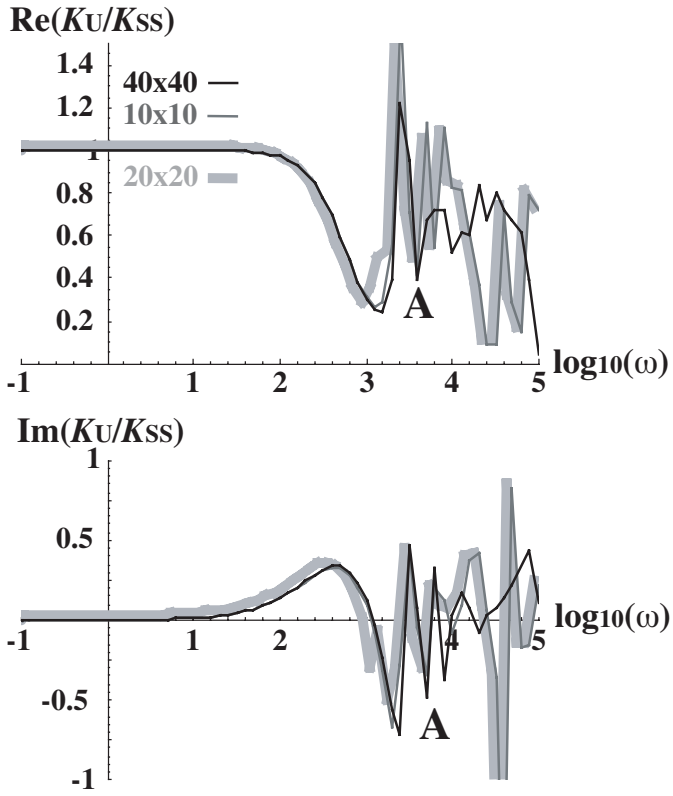

Real and imaginary parts of the normalized apparent permeability K_U/K_{SS} for networks with same total length (L = 1 m) and same mean radius (R = 100 μm) but different number of nodes (thin, black line, 40x40; thin, dark grey line, 10x10). The thick, light grey line represents the response of 20x20 networks, in which the mean radius was suddenly increased by a factor of 3 at mid-length in the flow direction. The black and dark grey curves are nearly coincident up to the point labeled A and the light grey curve is fairly similar. Above point A the grey curves become nearly coincident while the black one is quite different (see text for more details).

Conclusions

1) AC flow of a compressible fluid through a deformable pipe, pipe network, and, by extension porous rock propagates as a wave.

2) Flow waves are interface wave traveling along the fluid-solid interface. They have significant dispersion and attenuation. They can be identified with Biot slow compressional wave.

3) The flow field can be greatly affected by wave reflections and interferences.

4) The characteristic length is the distance L between reflectors. In the Earth, L could represent the thickness of geological formations or the distance between fracture intersections, and, therefore, could range from tens of centimeters to hundreds of meters. Thus, they could have a significant effect on data recorded at seismic frequencies.